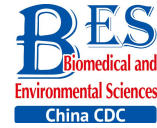# Original Article

Effects of Structural Changes in Subchondral Bone on Articular Cartilage in a Beagle Dog Model[*]

YAN Dong[1,2], LIU Tong Xi[2], LIU Bao Yue[3], WANG Ling[2], QIAN Zhan Hua[2], CHENG Xiao Guang[2,#], and LI Kun Cheng[1,#]

1. Department of Radiology, Xuanwu Hospital, Capital Medical University, Beijing 100053, China; 2. Department of Radiology, Beijing Jishuitan Hospital, Fourth Clinical Hospital of Peking University Health ScienceCenter, Beijing 100035, China; 3. Department of Pathology, Beijing Jishuitan Hospital, Fourth Clinical Hospital of Peking University Health Science Center, Beijing 100035, China

Abstract

Objective   Using MR T2-mapping and histopathologic score for articular cartilage to evaluate the effect of structural changes in subchondral bone on articular cartilage.

Methods   Twenty-four male Beagle dogs were randomly divided into a subchondral bone defect group (*n* = 12) and a bone cement group (*n* = 12). Models of subchondral bone defectin the medial tibial plateau and subchondral bone filled with bone cement were constructed. In all dogs, the left knee joint was used as the experimental sideand the right knee as the sham side. The T2 value for articular cartilage at the medial tibial plateau was measured at postoperative weeks 4, 8, 16, and 24. The articular cartilage specimens were stained with hematoxylin and eosin, and evaluated using the Mankin score.

Results   There was a statistically significant difference (*P* < 0.05) in Mankin score between the bone defect group and the cement group at postoperative weeks 16 and 24. There was a statistically significant difference in the T2 values between the bone defect group and its sham group (*P* < 0.05) from week 8, and between the cement group and its sham group (*P* < 0.05) from week 16. There was significant difference in T2 values between the two experimental groups at postoperative week 24 (*P* < 0.01). The T2 value for articular cartilage was positively correlated with the Mankin score (*ρ* = 0.758, *P* < 0.01).

Conclusion   Structural changes in subchondral bone can lead to degeneration of the adjacent articular cartilage. Defects in subchondral bone cause more severe degeneration of cartilage than subchondral bone filled with cement. The T2 value for articular cartilage increases with the extent of degeneration. MR T2-mapping images and the T2 value for articular cartilage can indicate earlycartilage degeneration.

Key words: MR T2-mapping; Subchondral bone; Articular cartilage; Degeneration

[#]Correspondence should be addressed to LI Kun Cheng and CHENG Xiao Guang, Tel: 86-10-58516688-6196, E-mail: cjr.likuncheng@vip.163.com and xiao65@263.net

Biographical note of the first author: YAN Dong, male, born in 1980, attending doctor, majoring in radiological medicine.

INTRODUCTION

Osteoarthritis (OA) is a chronic degenerative disease involving multiple joints of the body, but mainly involves the load-bearing joints such as the knees, hips, and ankles. Degeneration of articular cartilage is a key feature of OA. The extent of degeneration is related to the severity of the disease. Many studies have focused on changes in the articular cartilage but few have considered the subchondral bone. Recent studies have shown that subchondral bone undergoes enhanced remodeling in the early stages of OA. In addition, thickening and sclerosis of subchondral bone plays an important role in the development and progression of OA. Most notably, structural changes in subchondral bone have an important impact on degeneration of the articular cartilage. Some researchers believe that calcified cartilage and micro-injury in subchondral bone may be the factors that initiate bone remodeling[1] and that changes in subchondral bone have already occurred prior todegeneration of articular cartilage in the early stages of OA[2-5]. Another perspective is that the damage to cartilage occurs prior to changes in the subchondral bone. Sclerosis of subchondral bone may be a result of articular cartilage injury[6-8]. To date, no definite causal relationship has been identified between changes in subchondral bone and degeneration of articular cartilage during the progression of OA[9-11]. However, it is evident that remodeling of subchondral bone has important implications for the development and progression of degeneration of articular cartilage.

It is difficult to perform studies of the pathology or biomechanics of affected joints because of the relatively large interindividual differences in OA. Therefore, the pathophysiology of OA needs to be determined using an animal model[12]. Magnetic resonance (MR) imaging is a noninvasive screening method with high resolution that not only reveals morphologic changes in cartilage but also reflects the associated pathophysiologic processes involved. Thus, it is considered to be the best imaging method for articular cartilage[13]. Conventional MR imaging can show morphologic changes in articular cartilage, such as cracks or damage to the cartilage surface. However, it is insensitive to changes in the chemical composition of the extracellular matrix and in the structure of the collagen network in articular cartilage. Prior to development of damage visible to the naked eye, the chemical composition and mechanical properties of articular cartilage have already started to change. The advent of quantitative MR detection methods has made it possible to detect changes in the biochemical composition of cartilage prior to development of any visible morphologic changes. The transverse relaxation time (T2) of cartilage is a sensitive indicator of early degeneration of cartilage. It is particularly sensitive to changes in water content, collagen content, and anisotropy of collagen fibers in cartilage.

The aim of this study was to evaluate articular cartilage after structural changes in the subchondral bone using quantitative MR technology and pathologic analysis.

MATERIAL AND METHODS

Experimental Subjects

Twenty-four male Beagle dogs (age 12-13 months, weight 6-8 kg, from Laboratory Animal Center, Academy of Military Medical Sciences, China) were subjected to bilateral knee X-ray examinations prior to surgery to confirm that epiphyseal plates had been closed and no other joint disorders were present. The dogs were bred in the Animal Laboratory of Beijing Jishuitan Hospital and underwent the experimental surgery there. The dogs were caged individually under specific pathogen-free (SPF) conditions in the Laboratory Animal Research Center of Beijing Jishuitan Hospital at a temperature of 16-28 °C and a relative humidity of 40%-70% and artificially illuminated on an approximate 12-h light/dark cycle. The cage's floor area and height were 2 m^2 and 1.5 m, respectively. The air exchange rate was approximately 15 times per hour. All the dogs were provided with food and sterile water ad libitum, and walked 1.5 h 3 times per day. All the laboratory animals' requirements of environment and housing facilities were conducted in accordance with the State Standard of the People's Republic of China (GB 14928-2010). The Animal Welfare & Ethical Committee of Beijing Jishuitan Hospital approved the experimental protocol.

Animal Model

The dogs were randomly divided into two groups, i.e., a subchondral bone defect group (n = 12) and a bone cement group (n = 12) and subdivided

further into four time periods for assessment, i.e., 4, 8, 16, and 24 weeks (*n* = 3 each). The left knee joint of each dog was used as the experimental side and the right knee as the sham side (placebo surgery). The dogs were anesthetized with an intramuscular injection of Zoletil 50 (4 mg/kg) (Virbac Corporation, France) and Dexdomitor 25 µg/kg (Orion Corporation, Orion Pharma Espoo site, Finland) and placed in the supine position on the operating table. The fur was shaved locally on the left side of the knee and the skin prepared. Conventional sterilization techniques and sterile covers were used. An approximately 3-cm long longitudinal incision was made at the medial tibial plateau. The skin, subcutaneous tissues, and muscles were dissected to expose the medial tibial plateau, taking care to ensure the knee capsule was not damaged in the process. Under the computed tomography (CT) guidance, a ring drill with an outer diameter of 10 mm and an inner diameter of 9.5 mm was used to drill on the lateral side of the medial tibial plateau parallel to the articular surface. A curette was used to remove free and cancellous bone tissue remaining within the drilled hole. Finally, a cylindrical defect area measuring 10 mm in diameter and 10 mm in depth was established (Figure 1). By the CT positioning, the subchondral bone was scraped away as much as possible without involvement of the articular cartilage and the defect area was close to the articular surface of the tibial plateau, with a minimal distance of 2 mm away from the lower edge of the articular cartilage. For the bone cement group, cement powder (methylmethacrylate-methylacrylate copolymer powder, zirconium oxide powder, benzoyl peroxide) and liquid (methylmethacrylate, N,N-dimethylaniline,

p-phenylenediamine, and a small amount of chlorophyll VIII) were mixed together in the ratio of 2:1. The bone cement mixture (Refobacin Palacos R 40, Zimmer Biomet, Warsaw, IN, USA) was used to fill the cylindrical defect area. Finally, the layers of muscle, subcutaneous tissues, and skin were sutured and the wound was bandaged with gauze. The same longitudinal incision was made on the medial tibial plateau of the right knee but the subchondral bone defect modeling procedure was not performed, so that the right knees could serve as a sham surgery group. The bone defect modeling area was kept in contact with gauze bandages soaked in absolute ethanol for 10 min to prevent complete healing. The incision was then sutured and bandaged. After recovery from anesthesia, each animal was returned to its cage. An intramuscular injection of penicillin G (40,000 units/kg) was administered to each animal daily for the first 3 days after surgery. The surgical site was checked daily for signs of infection. All wounds had healed by 7-10 d postoperatively and the sutures could be removed. The dogs were not restricted on activity postoperatively. During the experiment, all the dogs were healthy and there was no dead.

CT Scanning and Positioning

The positioning images were acquired with an Aquilion 64-slice CT scanner (Toshiba Medical Systems, Tokyo, Japan). The scanning parameters include: section thickness 0.5 × 64 mm, matrix 512 × 512, pitch 0.828, tube voltage 120 kV, tube current 150 mA, field of view (FOV) 250 mm × 250 mm. The bone algorithm reconstruction was used and the coronal and sagittal images were obtained.
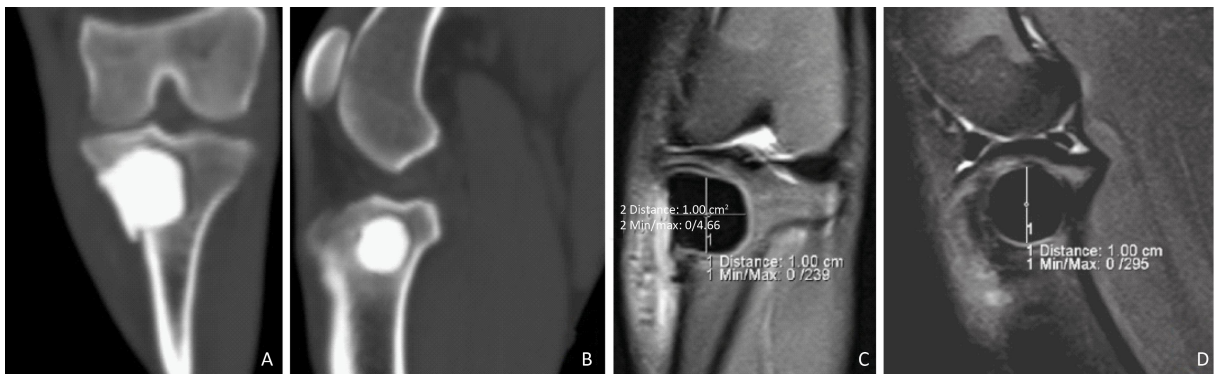

Figure 1. Experimental animals in the bone cement group. Creation of a subchondral bone defect model of the tibial plateau (left side) filled with bone cement. A. Computed Tomography (CT) scan, bone window, coronal plane. B. CT scan, bone window, sagittal plane. C. MR FS TSE PDWI, coronal plane, defect depth 10 mm. D. MR FS TSE PDWI, sagittal plane, defect diameter 10 mm.

MR Scanning and T2 Values for Articular Cartilage

MR scanning was performed at 4, 8, 16, and 24 weeks postoperatively in both the bone defect group and the cement group. All examinations were performed using an Espree 1.5T MR scanner (Siemens, München, Germany). The scans were performed using an 8-channel knee coil (Siemens). The dogs were anesthetized with an intramuscular injection of Zoletil 50 (4 mg/kg) and Dexdomitor (25 μg/kg) for the scans, and placed in a supine position on a custom-built experimental rack. The scanned knee was in an extended positionand kept parallel to the main magnetic field (B0).

Conventional sagittal and coronal scans were acquired using spin-echoT1 weighted imaging (T1WI), with a repetition time (TR) of 400 ms, and an echo time (TE) of 17 ms. The thickness of each layer was 3 mm and the layer spacing was 0 mm. The number of excitations was 1. The FOV was 10 cm × 10 cm and the matrix was 256 × 256. The scan time was approximately 3-4 min. Fat suppressed turbo spin-echo proton density weighted imaging (FS TSE PDWI) was used for scans in the sagittal plane at a TR of 3000 ms and a TE of 39 ms. The thickness of each layer was 3 mm and the layer spacing was 0 mm. The number of excitations was 2. The FOV was 10 cm × 10 cm and the matrix size was 218 × 256. The scan time was approximately 5-6 min.

For T2-mapping imaging and measurement of cartilage T2 relaxation time, a 6-echo spin-echo sequence was used for the sagittal plane scan at a TR of 1590 ms. The TEs were 15.8 ms, 31.6 ms, 47.4 ms, 63.2 ms, 79.0 ms, and 94.8 ms. The thickness of each layer was 3mm and the layer spacing was 0 mm. The number of excitations was 1. The FOV was 12 cm × 12 cm, the matrix was 320 × 320, and the band width was 150.0 Hz. The scan time was approximately 8-9 min.

The T2-mapping pseudocolor images of articular cartilage were taken, and the T2 value was measured in the region of interest in the articular cartilage in the sagittal images of the medial tibial plateau. Each cartilage specimen was divided into three (anterior, mid, posterior) sub-regions. The mid sub-region refers to the area of cartilage not covered by the meniscus. The T2 value was measured three times in each sub-region, and the average was taken as the T2 value of the region. The measurement of the T2 value for each cartilage specimen was performed by two radiologists and the results were tested for consistency.

Collection and Measurement of Cartilage Specimens

Dogs in the bone defect and bone cement groups were euthanized by veterinary compound ketamine overdose after the MR scans were completed at 4, 8, 16, or 24 weeks according to their allocated time group. The surrounding soft tissue of each knee joint was removed, the joint capsule was opened, and the anterior and posterior ligaments were removed. The internal meniscus and external meniscus were removed for observation of the color and shape of the articular cartilage in the tibial plateau, including whether there was any defect or damage present. The specimens were then fixed in 4% formaldehyde solution for histomorphological examination.

The formaldehyde-fixed specimens were decalcified in 10% neutral formaldehyde solution containing 10% ethylene diamine tetraacetic acid. The middle portion of the decalcified medial tibial plateau was embedded in paraffin and cut into 4 μm thick sagittal slices. The decalcified paraffin-embedded slices were then stained with hematoxylin and eosin (HE) and evaluated using the modified Mankin scoring system for articular cartilage under a light microscope[14]. The higher the score, the more severe the degeneration of the articular cartilage. The total score possible ranged from 0 to 14 points. Each HE-stained cartilage sample was scored by two pathologists and the results were tested for consistency. The mean of the two scores was used as the Mankin score of the sample.

Statistical Analysis

All data are shownas the mean ± standard deviation and were analyzed using SPSS version 17.0 software (SPSS Inc., Chicago, IL, USA). For repeated measurements, the intraclass correlation coefficient (ICC) was used to evaluate the repeatability and consistency of the data. The Shapiro-Wilk (W) test was used to checkthe parametersfor normal distribution. The paired-samples t-test was used to compare the T2 values between the bone defect group or the cement group and the corresponding sham group. The independent-samples t-test was used to compare T2 values between the bone defect group and the cement group in the same time period. The Wilcoxon test was used to compare the Mankin scores between the bone defect group or the cement group and the corresponding sham group. The Mann-Whitney U test was used to compare the Mankin scores between the bone defect group and

the cement group in the same time period. The Spearman correlation coefficient was used to measure the correlation between the T2 value of articular cartilage and its Mankin score. A *P*-value < 0.05 was considered to be statistically significant.

RESULTS

Visual Observation of Articular Cartilage Morphology

The articular cartilage of the tibial plateau was smooth in the bone cement and bone defect groups and in the corresponding sham surgery groups (Figure 2A). In the bone cement group, the articular surface of the tibial plateau was smooth at 4, 8, and 16 weeks postoperatively. However, rough patches containing small granules were observed on the medial articular surface at 24 weeks postoperatively. In the bone defect group, the articular cartilage surface was smooth at 4 and 8 weeks postoperatively (Figure 2B). While the surface remained relatively smooth at 16 weeks, rough patches containing small granules started to appear on the articular surfaceat this time (Figure 2C). At 24 weeks postoperatively, large defects were seen on the medial articular surface (Figure 2D).

Morphological Observation of Articular Cartilage by HE Staining and Mankin Scores

The average of the Mankin scores given by the two pathologists was used as the score for the sample (ICC0.983, indicating good consistency). Paraffin samples from all the sham groups showed relatively normal articular cartilage. The morphology of the articular cartilage at 4, 8, 16, and 24 weeks postoperatively was analyzed by HE staining (Figure 3A-3H). For the four time periods, the Mankin scores were 4.5 ± 0.5, 7.2 ± 1.0, 10.2 ± 1.2, and 12.3 ± 1.0, respectively, in the bone defect group and 4.0 ± 0.8, 5.8 ± 1.0, 6.8 ± 1.2, and 8.7 ± 1.0, respectively, in the bone cement group. The Mankin scores increased in both groups with the increasing of time (Table 1). When compared with the corresponding sham groups, there were significant differences in Mankin score between the bone defect group and the cement group (*P* < 0.05) at 8, 16, and 24 weeks postoperatively. There was a significant difference in Mankin score between the bone defect group and the bone cement group at 16 and 24 weeks postoperatively (*P* < 0.05).

T2 Value of Articular Cartilage

Pseudocolor T2 images showed the normal articular cartilage of the tibial plateau to have a smooth and continuous appearance, with a lower color scale and homogeneous signals (Figure 4A). Degeneration of articular cartilage was indicated by a focal or overall increase in the color scale, which could be uneven. Focal areas of increased color scale could be observed (Figure 4B-4D). The T2 values for the anterior, mid, and posterior cartilage areas were shown in Table 2 in the bone defect group and bone cement group.

In the bone defect group, the T2 value for the posterior articular cartilage (40.7 ± 1.3 ms) at postoperative week 4 was increased significantly when compared with its sham group (*P* < 0.05). The
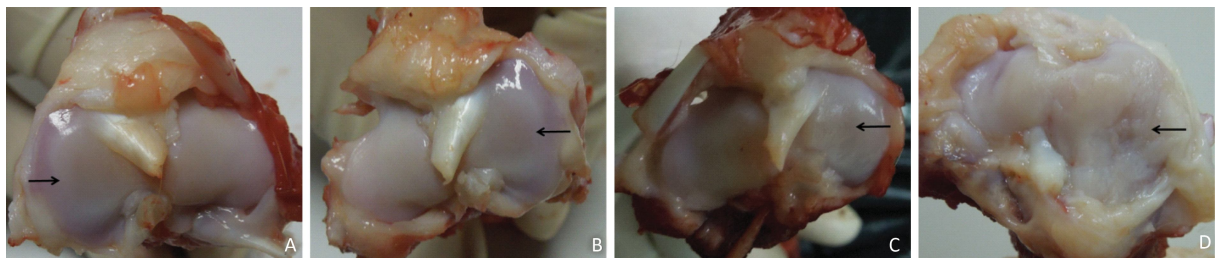

Figure 2. Representative tibial specimen at different time points postoperatively. A. In the bone defect group, at 4 weeks postoperatively, the sham side shows normal articular cartilage that is smooth in appearance (black arrow). B. In the bone defect group, 4 weeks postoperatively, the experimental side shows normal articular cartilage that is smooth in appearance (black arrow). C. In the bone defect group, at 16 weeks postoperatively, the experimental side shows rough patches containing small granules appearing on the surface of the articular cartilage (black arrow). D. In the bone defect group, at 24 weeks postoperatively, large areas of damaged articular cartilage can be seen on the experimental side (black arrow).

Table 1. Modified Mankin Scores in the Bone Defect Group and the Bone Cement Group

Postoperative Week	Bone Defect Group	Sham Group	Z	P-value	Bone Cement Group	Sham Group	Z	P-value	Z△	P△
4	4.5 ± 0.5	2.0 ± 0.6	-1.841	0.066	4.0 ± 0.8	2.2 ± 0.5	-1.604	0.109	-1.517	0.129
8	7.2 ± 1.0	1.8 ± 0.8	-2.032	0.042	5.8 ± 1.0	2.5 ± 0.8	-2.060	0.039	-1.888	0.059
16	10.2 ± 1.2	2.5 ± 0.5	-2.023	0.043	6.8 ± 1.2	2.0 ± 0.8	-2.023	0.043	-2.309	0.021
24	12.3 ± 1.0	2.8 ± 0.5	-2.041	0.041	8.7 ± 1.0	2.3 ± 0.6	-2.041	0.041	-2.309	0.021

Note. Z and P represent comparisons between the bone defect group or the cement group and the corresponding sham group using the Wilcoxon test. $Z^{\triangle}$ and $P^{\triangle}$ represent comparisons between the bone defect group and the cement group in the same time period using the Mann-Whitney U test.
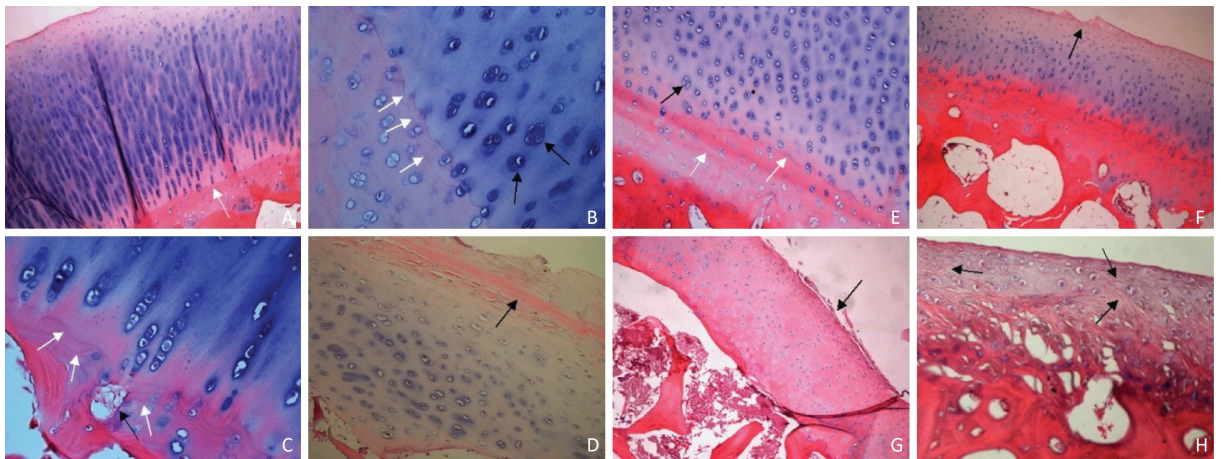

Figure 3. HE staining of articular cartilage. A. In the bone cement group, at 4 weeks postoperatively, there was no obvious abnormity in articular cartilage. The chondrocytes in the lower layers have a long columnar arrangement. HE staining of the cartilage matrix was blue with a clear continuous tide line (white arrow) (HE × 10). B. At 8 weeks postoperatively, chondrocytes on the experimental side have a disordered arrangement. Multiple tide lines (white arrows) and clusters of chondrocytes (black arrows) can be seen in the deeper layers (HE × 40). C. At 16 weeks postoperatively, multiple tide lines appear on the experimental side (white arrows) along with vascular invasion tide lines (black arrow) (HE × 40). D. At 24 weeks postoperatively, fibrosis of the cartilage surface is observed on the experimental side (black arrow). There is also a significant reduction in the number of chondrocytes present. The tide line has disappeared with a marked reduction instaining of the cartilage matrix (HE × 20). E. In the bone defect group, at 4 weeks postoperatively, the number of chondrocytes has extensively increased on the experimental side. Multiple tide lines (white arrows) and clusters of chondrocytes (black arrow) may be seen and the extent of cartilage matrix staining is mildly decreased (HE × 20). F. At 8 weeks postoperatively, small defects appear on the surface of the cartilage on the experimental side (black arrow). The arrangement of the cells is disordered and the extent of cartilage matrix staining is moderately decreased. Multiple tide lines have appeared (HE × 10). G. At 16 weeks postoperatively, fibrosis of the cartilage surface is observed on the experimental side (black arrow). There is also a significant reduction in the number of chondrocytes present. The cells have smaller nuclei with reduced cytoplasm. The tide line has disappeared, with a marked reduction in staining of the cartilage matrix (HE × 10). H. At 24 weeks postoperatively, thinner layers of cartilage are observed on the experimental side. The normal cartilage layers have disappeared and there is severe fibrosis of the cartilage matrix (black arrows). The number of chondrocytes is significantly decreased and the tide line has disappeared (HE × 20). Abbreviation: HE, hematoxylin and eosin.

T2 values for the mid and posterior cartilage were 39.6 ± 1.0 ms and 43.5 ± 2.9 ms, respectively, at postoperative week 8 and 43.1 ± 1.3 ms and 44.7 ± 0.2 ms at postoperative week 16; these values were significantly different from the corresponding sham groups ($P < 0.05$). At postoperative week 24, the T2 values for the anterior, mid, and posterior cartilage areas (39.6 ± 0.3 ms, 47.1 ± 2.8 ms, 48.4 ± 2.1 ms, respectively) were significantly different from those in their corresponding sham groups ($P < 0.05$).

In the bone cement group, the T2 values for the anterior, mid, and posterior cartilage areas were not significantly different ($P > 0.05$) from those in the corresponding sham group at postoperative weeks 4 (32.7 ± 2.1 ms, 36.0 ± 1.5 ms, 36.5 ± 6.1 ms, respectively) and 8 (35.2 ± 1.9 ms, 39.6 ± 2.7 ms, 39.8 ± 1.6 ms). However, the T2 values for the mid and posterior cartilage areas in the bone cement group were significantly different ($P < 0.05$) from those in the corresponding sham group at postoperative weeks 16 (42.1 ± 0.8 ms, 43.5 ± 1.9 ms) and 24 (43.6 ± 0.9 ms, 43.0 ± 1.8 ms).

Table 2. T2 Values (ms) for Articular Cartilage in the Bone Defect Group and Bone Cement Group

Postoperative Week	Anterior	Mid	Posterior	Anterior	Mid	Posterior	P^1	P^2	P^3
	Bone defect group			Sham group					
4	32.8 ± 1.3	33.2 ± 2.3	40.7 ± 1.3	33.1 ± 2.9	34.4 ± 8.2	35.6 ± 2.6	0.771	0.865	0.020
8	36.6 ± 1.3	39.6 ± 1.0	43.5 ± 2.9	35.2 ± 3.5	35.7 ± 1.6	37.5 ± 1.8	0.366	0.016	0.024
16	37.9 ± 2.6	43.1 ± 1.3	44.7 ± 0.2	34.4 ± 0.8	37.4 ± 0.2	36.2 ± 1.2	0.076	0.017	0.006
24	39.6 ± 0.3	47.1 ± 2.8	48.4 ± 2.1	35.3 ± 0.9	38.4 ± 0.5	38.4 ± 1.7	0.006	0.042	0.001
	Bone cement			Sham group					
4	32.7 ± 2.1	36.0 ± 1.5	36.5 ± 6.1	32.1 ± 1.1	31.4 ± 6.5	36.6 ± 1.2	0.787	0.365	0.988
8	35.2 ± 1.9	39.6 ± 2.7	39.8 ± 1.6	33.7 ± 1.9	36.7 ± 1.5	37.4 ± 3.3	0.184	0.296	0.129
16	37.1 ± 0.3	42.1 ± 0.8	43.5 ± 1.9	36.3 ± 3.0	36.7 ± 1.1	38.1 ± 1.3	0.705	0.027	0.045
24	39.8 ± 1.7	43.6 ± 0.9	43.0 ± 1.8	36.6 ± 1.7	36.6 ± 1.7	37.2 ± 2.2	0.113	0.006	0.011

Note. T2 values are reported as milliseconds. P^1, P^2, and P^3 refer to differences in T2 values between the anterior, mid, and posterior sub-regions of articular cartilage and their corresponding sham values in the bone defect group and the bone cement group (paired-samples *t*-test).
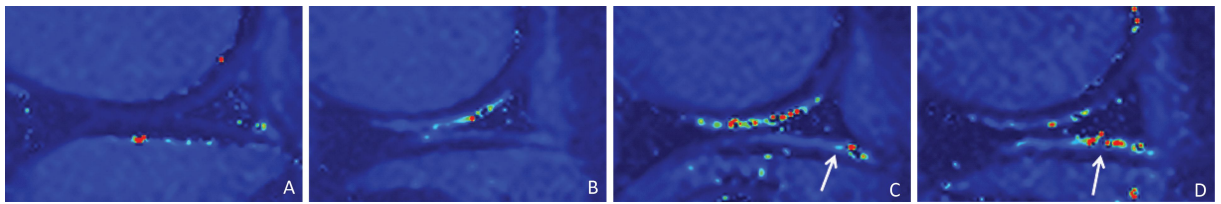

Figure 4. Magnetic resonance T2-mapping pseudocolor images of sagittal cartilage in the canine knee. A. In the bone cement group, at 8 weeks postoperatively, the sham side shows normal cartilage with a smooth and continuous articular surface. The color scale is relatively low and the signals are homogenous. B. In the bone cement group, at 8 weeks postoperatively, the experimental side shows an overall increase in color scale across the articular cartilage of the tibial plateau. The color scale is not uniform. C. In the bone cement group, at 24 weeks postoperatively, the experimental side shows an overall increase of color scale across the articular cartilage of tibial plateau. The color scale is not uniform and is focused in the posterior (white arrow). D. In the bone defect group, at 24 weeks postoperatively, the experimental side shows an overall increase incolor scale across the articular cartilage of the tibial plateau. The color scale is not uniform and is focused in the posterior (white arrow).

The mean T2 value for the three sub-regions of articular cartilage was taken as that of the articular cartilage (ICC 0.963, indicating good consistency). The results are shown in Table 3. In the bone defect group, the T2 values for articular cartilage at postoperative weeks 8, 16, and 24 were 35.6 ± 0.7 ms, 39.9 ± 1.6 ms, 41.9 ± 0.9 ms, and 45.0 ± 0.7 ms, respectively, and were significantly different from those in the corresponding groups ($P < 0.05$). In the bone cement group, the T2 values for articular cartilage were 35.1 ± 1.1 ms, 38.2 ± 1.6 ms, 40.9 ± 1.3 ms, and 42.1 ± 0.7 ms at postoperative weeks 4, 8, 16, and 24, respectively; the values at postoperative weeks 16 and 24 were significantly different from those in the corresponding sham groups ($P < 0.05$). There was no significant difference ($P > 0.05$) in T2 values between the bone cement and bone defect groups at postoperative weeks 4, 8, and

Figure 5. Correlation between T2 value and Mankin score in the bone defect group and the cement group (ρ = 0.758, $P < 0.01$, Spearman's test).

16. However, there was a significant difference at postoperative week 24 ($P < 0.01$, Table 3). The relationship between T2 values for articular cartilage and their corresponding Mankin scores in the bone defect group and the bone cement group is shown in Figure 5. There was a statistically significant correlation between the two (ρ = 0.758, $P < 0.01$, Spearman's test for non-normally distributed samples).

DISCUSSION

The subchondral bone includes the dense subchondral bone plate and its spongy trabecular bone. The main role of the subchondral bone is to absorb, mitigate, and transmit the force that the joint has to bear, as well as maintain the morphology and physiologic microenvironment of the joint. Subchondral bone also provides nutrition for the deeper layers of cartilage and plays an important role in maintaining normal joint function.

Male Beagle dogs were chosen for this experiment to avoid the effect of estrogen on cartilage in this animal model of OA[15-16]. An extra-articular surgical model was used to preserve the integrity of the joint and to avoid the interference of synovial inflammation caused by intra-articular surgery. The subchondral bone of the medial tibial plateau was scraped in the bone defect and bone cement groups, which resulted in damage to its structure and weakened the ability of the subchondral bone to absorb, disperse, and transmit the forceapplied via the articular cartilage. In addition, the vascular network of the subchondral bone area was damaged, which reduced its abilityto supply nutrients to the deeper layers of cartilage. Thus,
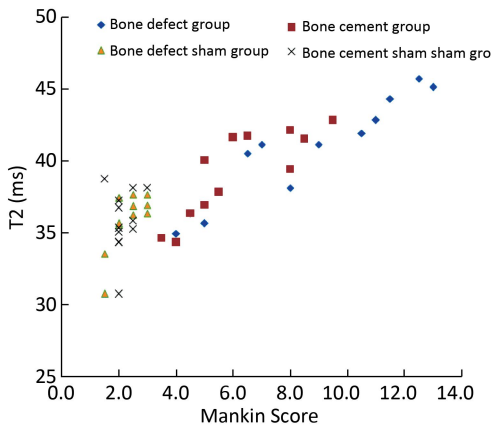
Table 3. T2 Values for Articular Cartilage in the Bone Defect Group and the Bone Cement Group

Postoperative Week	Bone Defect Group	Sham Group	*P*-value	Bone Cement Group	Sham Group	*P*-value	$P^{\triangle}$
4	35.6 ± 0.7	34.4 ± 3.2	0.583	35.1 ± 1.1	33.4 ± 2.4	0.236	0.512
8	39.9 ± 1.6	36.1 ± 2.3	0.013	38.2 ± 1.6	35.9 ± 2.0	0.058	0.269
16	41.9 ± 0.9	36.0 ± 0.4	0.004	40.9 ± 1.3	37.1 ± 1.5	0.037	0.313
24	45.0 ± 0.7	37.4 ± 0.4	0.004	42.1 ± 0.7	36.7 ± 1.6	0.011	0.006

Note. T2 values are reported as milliseconds. *P* denotes comparison between the bone defect/cement group and the corresponding sham group (paired-samples *t*-test). $P^{\triangle}$ denotes comparison between the bone defect group and the cement group for the same time period (independent-samples *t*-test).

the metabolic activity of the chondrocytes was also affected. Any subchondral bone defects or defects filled by bone cement will cause degeneration of articular cartilage[17-19]. In the bone defect group, the subchondral bone was severely damaged, which significantly weakened its ability to support the articular cartilage, mitigate force, and supply nutrients to the deeper layers of cartilage. Consequently, there was significant degeneration of the articular cartilage. Whilst the cement group to a certain extent has supported the articular cartilage, and buffered its force; however, its ability to mitigate force applied via the articular cartilage is still less than that found in healthy trabecular bone, and degeneration of articular cartilage still occurred, albeit to a lesser extent than in the bone defect group. Flassica et al.[20] found that subchondral bone filled with polymethylmethacrylate did not affect articular cartilage. However, their subchondral bone samples were approximately 6-9 mm thick. Some of the subchondral bone was retained in their study, soit is possible that the impact of bone cement on articular cartilage was weakened. In this study, the remaining bone plate was about 2 mm thick, and the trabecular bone structure was almost completely destroyed. Thus, bone cement has an effect on the articular cartilage.

MR T2-mapping uses a multi-echo spin-echo pulse sequence to measure MR signal intensity at different echo times, and then perform nonlinear calculation and get pseudocolor imaging[21-22]. This reflects the spatial distribution of the T2 value in the articular cartilage; from this, the T2 value of the region of interest in the cartilage was obtained. The T2 value of articular cartilage is closely related to the water content in the cartilage matrix, the collagen content, and the anisotropic arrangement of collagen fibers[23-26].

At all four time points in our study, the cartilage T2 values in the two experimental groups tended to be higher than those in their corresponding sham groups. From postoperative week 8 onwards, there was a statistically significant difference in the T2 value between the bone defect group and its sham group. There was also a statistically significant difference inthe T2 value between the bone cement group and its sham group at 16 weeks postoperatively. The structure of the subchondral bone was severely damaged and its function impaired in the bone defect group, whereas the bone cement preserved the support and buffering functions of the subchondral bone in the cement group. Hence, the bone defect group developed significantly different T2 values compared to its corresponding sham group earlier than the bone cement group. While there were no significant differences in T2 values of the bone defect group at 4 weeks and bone cement group at 8 weeks compared with their corresponding sham groups, the articular cartilage started to show a heterogeneous increase in color scale on the T2-mapping pseudocolor images, indicating early degeneration of articular cartilage. The main factors that influence the T2 value of cartilage are its water content, collagen content, and structural integrity. Cracks appear on the articular cartilage surface when the structural integrity of the cartilage is damaged. As the degenerative process continues, the fissures deepen and progress to cartilage defects[27-29]. When this happens, the content of collagen in the cartilage matrix continues to decrease, and the structural network is gradually destroyed, with disappearance of anisotropy and an increase in T2 value. At the same time, there is a change in the water content of the cartilage; an increase is seen in the early stages of degeneration and a decrease later on. The increased Mankin score for articular cartilage in our study indicated progressive degeneration. Thus, the increase in the cartilage T2 value can indicate degeneration of articular cartilage.

Our study has some limitations. In the early postoperative weeks of the study, although the T2 values in the experimental groups showed an increasing trend compared with their corresponding sham groups, the differences were not statistically significant, which may be attributed to the small sample size. Whilst cartilage MR T2-mapping can indicate early degeneration of articular cartilage, there are several other factors, including the 'magic angle' effect and chemicalshift artifacts, that can affect the results[6]. In addition, the longest observation period in our study was 6 months after surgery, which could be extended further in future research to assess the long-term effects of structural changes in subchondral bone on articular cartilage.

In summary, structure changes in subchondral bone can lead to varying degrees of degeneration in articular cartilage. MR T2-mapping can be used for noninvasive and quantitative analysis of changes in the articular cartilage at a molecular level. It is a sensitive method for early detection of cartilage degeneration, and can detect changes in the composition and structure of cartilage before any marked morphologic changes have occurred[30].

When treating related diseases, any impact on subchondral bone should be avoided or minimized. When the structure of the subchondral bone is damaged, an appropriate filling material can be used to repair the damage and restore its function. To a certain extent, this approach can reduce the negative impact on articular cartilage and reduce the severity of degeneration. This study has provided a basis for the clinical treatment of subchondral bone-related diseases along with a new method for studying the pathogenesis of OA and its treatment.

REFERENCES

1. Pastoureau PC, Chomel AC, Bonnet J. Evidence of early subchondral bone changes in the meniscectomized guinea pig. A densitometric study using dual-energy X-ray absorptiometry subregional analysis. Osteoarthritis Cartilage, 1999; 7, 466-73.

2. Guo WS, Li ZR, Cheng LM, et al. The effect of subchondral bone defect in femoral head on structure and metabolism of article cartilage. Natl Med J China, 2008; 88, 2795-8.

3. Hisatome T, Yasunaga Y, Ikuta Y, et al. Effects on articular cartilage of subchondral replacement with polymethylmethacrylate and calcium phosphate cement. J Biomed Mater Res, 2002; 59, 490-8.

4. Zuo Q, Lu S, Du Z, et al. Characterization of nano-structural and nano-mechanical properties of osteoarthritic subchondral bone. BMC Musculoskeletal Disord, 2016; 17, 367.

5. Zamli Z, Robson Brown K, Sharif M. Subchondral bone plate changes more rapidly than trabecular bone in osteoarthritis. Int J MolSci, 2016; 17, 1496.

6. Mosher TJ, Smith H, Dardzinski BJ, et al. MR imaging and T2 mapping of femoral cartilage: *in vivo* determination of the magic angle effect. Am J Roentgenol, 2001; 177, 665-9.

7. Day JS, Ding M, van der Linden JC, et al. A decreased subchondral trabecular bone tissue elastic modulus is associated with pre-arthritic cartilage damage. J Orthop Res, 2001; 19, 914-8.

8. Ding M, Odgaard A, Hvid I. Changes in the three-dimensional microstructure of human tibial cancellous bone in early osteoarthritis. J Bone Joint Surg Br, 2003; 85, 906-12.

9. Pan J, Wang B, Li W, et al. Elevated cross-talk between subchondral bone and cartilage in osteoarthritic joints. Bone, 2012; 51, 212-7.

10. Sharma AR, Jagga S, Lee SS, et al. Interplay between cartilage and subchondral bone contributing to pathogenesis of osteoarthritis. Int J Mol Sci, 2013; 14, 19805-30.

11. Findlay DM, Kuliwaba JS. Bone-cartilage crosstalk: a conversation for understanding osteoarthritis. Bone Research, 2016; 4, 16028.

12. Lahm A, Uhl M, Edlich M, et al. An experimental canine model for subchondral lesions of the knee joint. Knee Jan, 2005; 12, 51e5.

13. Kraus VB, Feng S, Wang S, et al. Subchondral bone trabecular integrity predicts and changes concurrently with radiographic and MRI determined knee osteoarthritis progression. Arthritis Rheum, 2013; 65, 1812-21.

14. Mankin HJ, Dorfman H, Lippiello L, et al. Biochemical and metabolic abnormalities in articular cartilage from osteo-arthritic human hips. II. Correlation of morphology with biochemical and metabolic data. J Bone Joint Surg Am, 1971; 53, 523-37.

15. Dietrich W HA, Holzer G, Huber JC, et al.Estrogen receptor-beta is the predominant estrogen receptor subtype in normal human synovial. J Soc Gynecol Investig, 2006; 13, 512-7.

16. Harri EP, Jyrki N, Jyrki JP, et al. Subchondral bone remodeling increases in early experimental osteoarthrosis in young beagle dogs. Acta Orthopaedica, 1998; 69, 627-32.

17. Tomoya M, Hiroshi H, Toru O, et al. Role of Subchondral Bone in Osteoarthritis Development, A Comparative Study of Two Strains of Guinea Pigs With and Without Spontaneously Occurring Osteoarthritis, Arthritis& Rheumatism, 2007; 56, 3366-74.

18. Andreas HG, Henning M, Gunnar K, et al. The subchondral bone in articular cartilage repair: current problems in the surgical management. Knee Surg Sports Traumatol Arthrosc, 2010; 18, 434-47.

19. Kawcak CE, McIlwraith CW, Norrdin RW, et al. The role of subchondral bone in joint disease: a review. Equine Vet J, 2001; 33, 120-6.

20. Frassica FJ, Gorski JP, Pritchard DJ, et al. A comparative analysis of subchondral replacement with polymethylmethacrylate or autogenous bone grafts in dogs. Clin Orthop Relat Res, 1993; 293, 378-90.

21. Xu L, Hayashi D, Roemer FW, et al. Magnetic resonance imaging of subchondral bone marrow lesions in association with osteoarthritis. Semin Arthritis Rheum, 2012; 42, 105-18.

22. Taylor C1, Carballido-Gamio J, Majumdar S, et al. Comparison of quantitative imaging of cartilage for osteoarthritis: T2, T1rho, dGEMRIC and contrast-enhanced computed tomography. Magn Reson Imaging, 2009; 27, 779-84.

23. Mosher TJ, Smith HE, Dardzinski BJ. MR Imaging and T2 mapping of femoral cartilage. Am J Roentgeno, 2012; 178, 1569-70.

24. Watrin-Pinzano A, Ruaud JP, Cheli Y, et al. T2 mapping: an efficient MR quantitative technique to evaluate spontaneous cartilage repair in rat patella. Osteoarthritis Cartilage, 2004; 12, 191-200.

25. Lazik-Palm A, Kraff O, Johst S, et al. Morphological and Quantitative 7 T MRI of hip cartilage transplants in comparison to 3 T-initial experiences. Invest Radiol, 2016; 51, 552-9.

26. Kang Y, Choi JA. T2 mapping of articular cartilage of the glenohumeral joint at 3.0 T in healthy volunteers: a feasibility study. Skeletal Radiol, 2016; 45, 915-20.

27. Atik OS. Is subchondral bone the crucial point for the pathogenesis and the treatment of osteoarthritis? Eklem Hastalik Cerrahisi, 2014; 25, 1.

28. Yuan XL, Meng HY, Wang YC, et al. Bone-cartilage interface crosstalk in osteoarthritis: potential pathways and future therapeutic strategies. Osteoarthritis Cartilage, 2014; 22, 1077-89.

29. Li G, Yin J, Gao J, et al. Subchondral bone in osteoarthritis: insight into risk factors and microstructural changes. Arthritis Res Ther, 2013; 15, 223.

30. Gray ML, Burstein D, Xia Y. Biochemical (and functional) imaging of articular cartilage J. Semin Musculoskelet Radiol, 2001; 5, 329-43.